

MEASUREMENT OF LOW-ENERGY PARTICLES
BY THE MARS-2 AND MARS-3 PLANETARY PROBES.
II..PRELIMINARY RESULTS

O.L. Vaysberg et al.

Translation of "Izmereniye chastits maloy energii na avtomaticheskikh mezhilanetnykh stantsiyakh 'Mars-2' i 'Mars-3'," Kosmicheksiyе issledovaniya, Vol. 11, No. 5, Sept-Oct 1973, pp. 743-755



(NASA-TT-F-15540) MEASUREMENT OF
LOW-ENERGY PARTICLES BY THE MARS-2 AND
MARS-3 PLANETARY PROBES. 2:
PRELIMINARY RESULTS (Kanner (Leo)
Associates) 24 p HC \$4.25

N74-22446

CSCI 03B

G3/30

Unclas
37015

NATIONAL AERONAUTICS AND SPACE ADMINISTRATION
WASHINGTON, D.C. 20546

APRIL 1974

STANDARD TITLE PAGE

1. Report No. NASA TT F-15,540	2. Government Accession No.	3. Recipient's Catalog No.	
4. Title and Subtitle MEASUREMENT OF LOW-ENERGY PARTICLES BY THE MARS-2 AND MARS-3 PLANETARY PROBES. II. PRELIMINARY RESULTS		5. Report Date April 1974	
		6. Performing Organization Code	
7. Author(s) O.L. Vaysberg, et al.		8. Performing Organization Report No.	
		10. Work Unit No.	
9. Performing Organization Name and Address Leo Kanner Associates, P.O. Box 5187, Redwood City, California 94063		11. Contract or Grant No. NASW-2481	
		13. Type of Report and Period Covered Translation	
12. Sponsoring Agency Name and Address NATIONAL AERONAUTICS AND SPACE ADMINIS- TRATION, WASHINGTON, D.C. 20546		14. Sponsoring Agency Code	
15. Supplementary Notes Translation of "Izmereniye chastits maloy energii na avtomaticheskikh mezhilanetnykh stantsiyakh "Mars-2" i "Mars-3", " Kosmicheskiye issledovaniya, Vol. 11, No. 5, Sept-Oct 1973, pp. 743-755.			
16. Abstract Data are presented on streams of charged particles with energy from 0.03 to 10 kev, obtained with Mars-2 and Mars-3 planetary probes in the solar wind during flight from Earth to Mars, in the Earth's geomagnetic trail and in the vicinity of Mars. The typical spectrum of undisturbed solar wind presented was made on 29 Jun 1971. Its calculated parameters are: velocity of solar wind 414 km/s, proton temperature 6.45 ev, α -particle temperature 24.3 ev, ratio of α -particle to proton concentration 2%. Calculated values of these parameters for all measurements made each 20 min from 26 Jun to 10 Jul 1971 are also graphically presented, as are histograms of solar wind velocity, temperature of protons and He^{++} ions, and ratios of He^{++} ion to proton concentration obtained from measurements between 16 Jun and 21 Aug 1971. Data are also included for measurements obtained in the Earth's geomagnetic trail, also shown on the Mars-3 trajectory graph. Anomalies of energy spectra were discovered close to Mars, to be explained by the disturbing influence of the planet. Analysis of energy spectra ions showed that a shock wave is formed during the interaction of solar wind with Mars. Ions of very low energy (~ 30 ev) were discovered 1000-2000 km from the planet, possibly of ionospheric origin.			
17. Key Words (Selected by Author(s))		18. Distribution Statement Unclassified - Unlimited	
19. Security Classif. (of this report) Unclassified	20. Security Classif. (of this page) Unclassified	21. No. of Pages 34	22. Price 4.25

MEASUREMENT OF LOW-ENERGY PARTICLES
BY THE MARS-2 AND MARS-3 PLANETARY PROBES.
II. PRELIMINARY RESULTS

O.L. Vaysberg et al.

One of the tasks of the Mars-2 and Mars-3 spacecraft ~~was to~~ 743* research into the plasma of solar wind during the flight from Earth to Mars and in the close vicinity of Mars when the satellite was orbiting the planet. This experiment had to be carried out since there was relatively little information on the properties of solar wind plasma at distances greater than 1.2 A.U., although attempts to carry out this measurement had been done earlier. In 1964, the American Mariner-4 spacecraft had been launched towards Mars, and contained an instrument for studying the characteristics of hot plasma [1]. However, malfunctioning meant that only a limited amount of reliable information was obtained from the instrument and the quality was poor. Therefore, it was not possible to obtain a complete answer to all the questions posed during preparation of the experiment, especially, to determine the characteristics of plasma flows near Mars.

However, magnetic measurement, carried out by the same spacecraft, was complete and a significant abrupt disturbance of the magnetic field was recorded in the close vicinity of Mars. The disturbance is similar to that which was observed in interplanetary shock waves, although it was impossible to give a simple answer, merely by magnetic data, as to whether this disturbance was caused by the planet or whether it was similar to disturbances which had been frequently observed before this in the interplanetary medium during the flight from Earth to Mars [2] (see also the discussion in work [3, 4]). Measurement conducted on Mariner-4 made it possible to give a high valuation to the dimension of the magnetic dipole moment of Mars ($2 \cdot 10^{-4}$ of

*Numbers in the margin indicate pagination in the foreign text.

that of Earth) and the dimensions of its magnetosphere [2, 3].

During subsequent flights to Mars in the Mariner series, /744
there was no equipment for measuring plasma characteristics and the magnetic field. However, measurements were made of atmospheric density and the electron concentration in the ionosphere by radio illumination. The profile of electron concentration in the ionosphere of Mars was obtained by this measurement [5]. The maximum electron concentration, $1.5 \cdot 10^{-5} \text{ cm}^3$, is attained at an altitude of 130-150 km; the characteristic scale of the ionosphere was 20-25 km. This amount of electron concentration gives sufficient electron pressure for the ionosphere to reduce the flow of solar wind and cause a boundary shock wave in the transition area. Results of these calculations, made by Spreiter et al. [4], give reason to suppose that the head of the shock wave is ~~1000 km~~ from the planet's surface.

In a number of works, the need is indicated to take into account the conductivity of flows in the atmosphere when investigating problems on solar wind around Mars (see, for example [6]). Therefore, before the Mars-2 and Mars-3 spacecraft were launched, there was only a limited amount of information on the interaction of solar wind on Mars and phenomena which accompany this. And an elongated elliptical orbit is the most suitable to measure plasma and the magnetic field. Here, one can carry out measurement at various altitudes and in various interaction areas, including at relatively short distances from the planet, where the boundary, disturbing the solar wind must lie.

Another very interesting possibility which arises when launching spacecraft to planets outside of the solar system is the study of the effects of the interaction of solar wind on the Earth's magnetosphere at great distances. A short time after launch, the vehicle is in an area beyond Earth below the

plasma flow. The first measurements of this type were carried out by the American Pioneer-7 and Pioneer-8 spacecraft at distances of 6 million and 3 million km, respectively [7, 8]. Instruments set up in these stations registered anomalous ion spectra where the tail was expected to be, and these differed substantially from ion spectra of solar wind. Apart from this, a significant decrease in flows to a level lower than the threshold of the instruments and uncorrelated variations of plasma flow and the magnetic field were recorded [9]. This was interpreted as the intersection of the Earth's plasma wake.

When Mars-2 and Mars-3 were on a flight to Mars, they passed this zone 2 months after launching at a distance of approximately 20 million km. Studying this phenomenon at significantly different distances, makes it possible to study the relaxation in solar wind plasma, and the possible reconnection of lines of force and the heating of plasma linked with them.

A third question which was studied during the flight was that of the dynamics of solar wind and geomagnetic activity linked with it. Up until now, measurement of solar wind between Earth and Mars orbits has only been done to a limited extent on Mariner-4 [1]. The first results of this measurement are shown in [9-13].

Measurement in the Solar Wind

Regular measurement of energy spectra of solar wind particles was done during the whole flight of the Mars-2 and Mars-3 spacecraft towards Mars. Electrostatic analyzers were switched on during the Earth-Mars course, basically at a frequency of three times per hour (on some parts of the course, this frequency was six times per hour). When the instrument was switched on once, measurement of two complete energy spectra was done. The time 1745 for obtaining one spectrum was 32 seconds. Two measurements

with an average count speed having a time interval of 3.5 sec was done for each spectrum on each energy stage. When two counts followed each other with a relatively short time interval on one and the same energy stage, it was possible to eliminate the effect of transient processes in an instrument, which were considerable when measuring small flows, during result processing.

Processing of spectra obtained was done on an electronic digital computer. Transient processes were calculated on the basis of the well-known transient characteristic of an instrument, on the supposition that during a time of 3.5 sec, the flow of solar wind particles would not significantly change.

An important aspect when studying solar wind is experimental research into all types of irregularities of particle flow. Rapidly changing (small-scale) disturbances must affect primarily the shape of energy spectra particles. Therefore, research into the shape of spectra and isolating the range of measurements was included in the program of machine processing of the results, where the occurrence of unusual spectra of positive ions, the shape of which was quite different from the well-known shape of the ion spectrum of an undisturbed solar wind, was observed.

As is known (see, for example, [14]), an ion spectrum of undisturbed solar wind, obtained by an electrostatic analyzer has several maxima on some part of the scale E/q (E = energy, q = particle charge), the relative position of which does not change with time. (For ease of identification in the future, we shall write E instead of E/q .) It is known that the main maximum (greatest in value) occurs when $E = E_0$, is caused by protons, with a maximum $E = 2E_0$ from He^{++} ions, and maxima with greater value E are found in heavy ions. When $E < E_0 - \Delta E$ (ΔE is the width of the main maximum) hardly any charged particles

were observed. Therefore, when analyzing spectra by signs, by which the spectrum ought to belong to a disturbed plasma, there were: a large relative width of the main maximum; flow values left of the main maximum, exceeding a certain threshold, linked with the presence of small energy particles, and also abnormally large flow values to the right of the main maximum, which could not be explained by the presence of α -particles or heavier ions. Only one of these signs listed above would be considered sufficient to include the spectrum as an "unusual" one.

In Fig. 1 is shown a typical spectrum of undisturbed solar wind, measured by the Mars-3 spacecraft. Examples of disturbed spectra can be seen below in Fig. 5. /746

The program for processing spectra envisaged the determination of the speed of solar wind, the temperature and concentration of protons and ions of helium for each measured spectrum (an arbitrary concentration was calculated, so that the instrument did not record a complete particle flow).

When calculating these parameters, the following approximations were made. It was considered that the main maximum in a spectrum of positively charged particles is caused by protons. The contribution of helium to readings of the power channel, closest to the maximum and situated to the right of it, was calculated according to the formula:

$$I_{He}(i_{max}+1) = \frac{E(i_{max}+1)}{E(i_{max}+3)} I(i_{max}+3), \quad (1)$$

where i_{max} is the number of the channel with a maximum reading; $I_{He}(i_{max}+1)$ is the contribution of He^{++} to the reading of the channel with a number $i_{max}+1$; $E(i)$ is the energy level (in protons) of the i -th channel; $I(i)$ is the reading of the i -th channel, i.e., the contribution of the low energy wing He^{++} to the high energy wing H^+ was taken as being equal to the reading

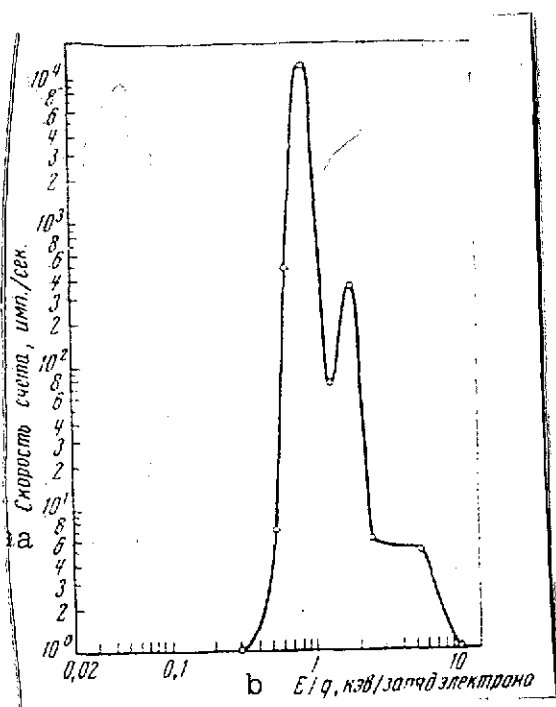


Fig. 1. A typical spectrum of undisturbed solar wind, measured by the Mars-3 spacecraft, 29 Jun 1971. The calculated value of parameters for this spectrum: speed of solar wind $V_0 = 414$ km/sec; proton temperature $T_p = 6.45$ ev; temperature of α -particles $T_\alpha = 24.3$ ev; ratio of concentration of α -particles to the concentration of protons $n_\alpha/n_p = 2\%$.

Key: a. Count speed, impulses/sec
b. E/q , kev/electron charge

in the high energy wing He^{++} . The coefficient when $I(i_{\max} + 3)$ in this very approximated formula takes into account the proportion of the energy window ΔE of energy E for an electrostatic analyzer.

The inaccuracy in the evaluation of relative contribution of ions of He^{++} and H^+ in the reading of the channel with number $i_{\max} + 1$, in the majority of cases does not introduce a significant error into determining the proton parameters, since the value (1) is small, but when determining the helium parameters, the error linked with this approximation is significant. Nevertheless, the values of helium parameters obtained by this simple method described here can be used for preliminary evaluation of the average values of these dimensions on a great number of spectra.

In order to calculate parameters, formulas were used obtained by assuming the convected isotropic Maxwellian distribution of particles. Here, for an electrostatic analyzer with a small angular factor¹, the reading in the i -th energy channel caused by protons is shown by the formula:

¹Formula (2) is justified for analyzers with an angular factor of $\Omega \ll 2T/E$. For analyzers used $\Omega \sim 3 \cdot 10^{-3}$ ster.

$$I_p(i) = \frac{\bar{S}\bar{\Omega}n_p}{\sqrt{2\pi m_p}} \frac{E_i^2}{T_p} e^{-\frac{(E_i - E_0)^2}{T_p}} - \frac{2(E_i + E_0)(1 - \cos \theta)}{T_p} \frac{\Delta E_i}{E_i} \quad (2)$$

where $I_p(i)$ is the reading on the i -th energy channel caused by protons; m_p is the mass of a proton; n_p is the concentration; T_p is the temperature of protons; E_0 is the energy of a proton moving with average mass velocity; E_i is the energy level; ΔE_i is the solution of the i energy channel; $\bar{\Omega}$ is the solid angle of the instrument; \bar{S} is the average angular transmission area; θ is the angle between the mass velocity vector and the normal to the plane of the input aperture of the instrument. The angle θ taken as being equal to the average angle of aberration.

If one takes the ratio of the currents in the two adjacent channels, from formula (2), after logarithmic operation, we shall obtain the linear function relative to T_p and E_0 . In this way, 748
 T_p and E_0 are determined by solving the linear equations obtained from the formulas for $I(i_{\max})/I(i_{\max} - 1)$ and $I(i_{\max})/I(i_{\max} + 1)$.

The formulas obtained for T_p and E do not depend on S , Ω and $\Delta E_i/E_i$. In this approximation, T_p also does not depend on the angle θ . The value of E_0 depends little on θ , and the value of concentration n_p depends significantly on this angle. As a result, the values of n_p obtained only characterize part of the flow entering the instrument, and are not a concentration of particles in the generally accepted sense, since they are subject to fluctuations, linked with changes in angle θ , which are not measured by the instrument.

The temperature of helium which was ionized twice T_{He} and the ratio of the coefficient of helium to the concentration of protons n_{He}/n_p were calculated similarly to the proton parameters. The average mass velocity of ions of He^{++} was assumed as equalling

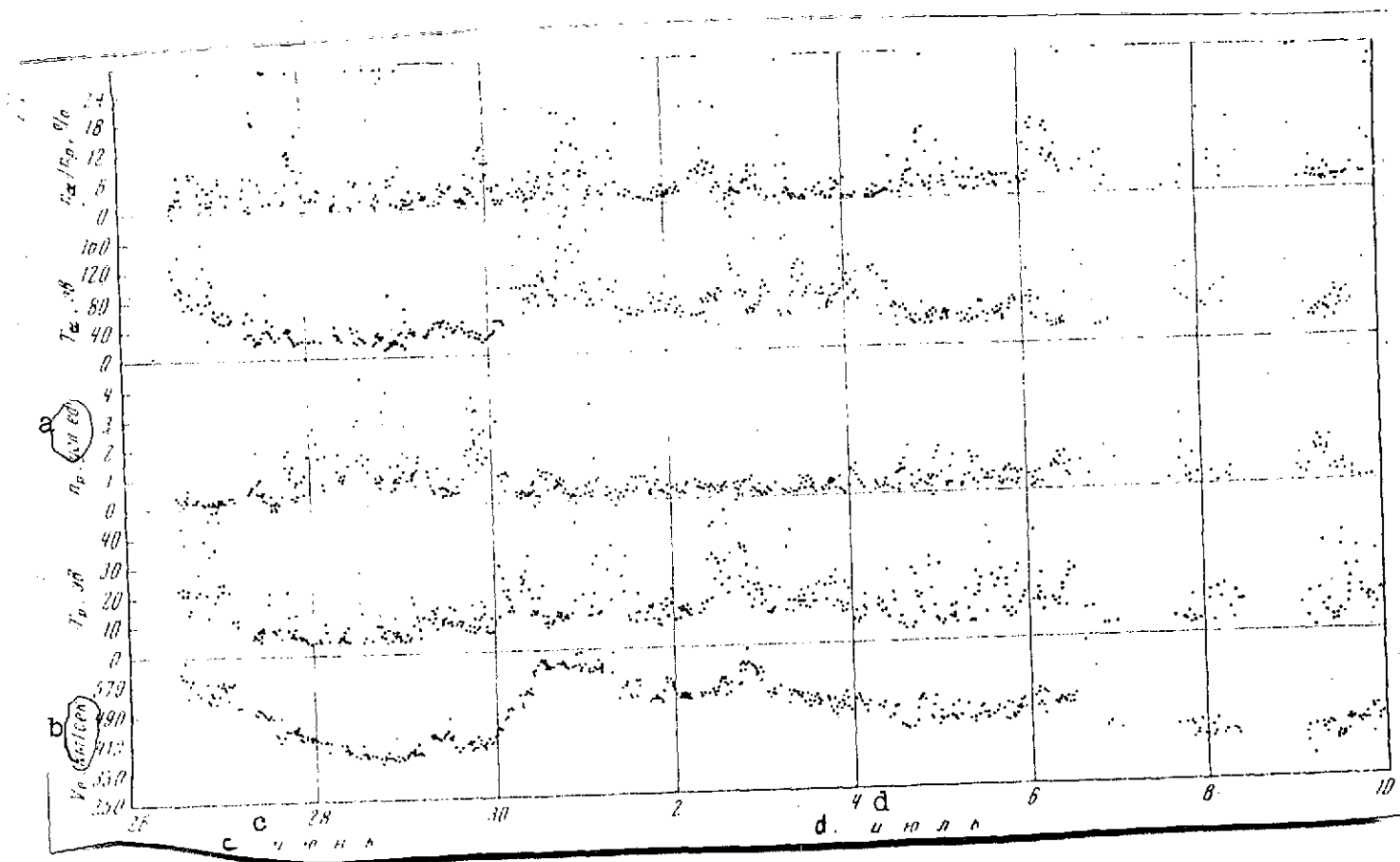


Fig. 2. Graphs of the calculated parameters of solar wind, obtained on the BESM-4 electronic computer, on measurement of solar wind, onboard the Mars-3 spacecraft from 26 Jun to 10 Jul 1971. Measurements are shown for every 20 minutes. Individual peaked traces of parameters, especially of n_{α}/n_p , are due to undetermined failures in the computer and the simplicity of the algorithm for calculating n_{α}/n_p .

Key: a. Nominal units; b. km/sec; c. June; d. July

the average velocity of protons. The contribution of protons into the readings of corresponding energy channels was calculated by formula (2) on the basis of the values which were found for parameters of a proton component.

The results of calculations of the parameters mentioned were issued for printing and recorded on magnetic tape for further processing. Apart from this, the values of the parameters obtained can be shown in the form of graphs, depending on the time, by using a camera attachment.

In Fig. 2, as an example, are shown graphs of parameters obtained by this method with measurements from 26 June to 10 July 1971. Each dot on the graph of the appropriate parameter was obtained by averaging its value with two adjacent spectra, measured during 1 minute. The time interval between the two closest dots equals 20 minutes.

7749

The values of n_p are given in nominal units, since it is impossible to give an accurate rating for them. As for the discussed dependence on angle θ , the interpretation in changes of parameters n_p must be done carefully. Nevertheless, it can be said that during time variations of n_p , in most cases, there is the well-known dependence between the concentration of particles and plasma velocity, consisting in the increase of concentration of rapid flow on the leading edge (see, for example, [15]).

The temperature of protons tends to increase with velocity; therefore, temperature peaks often occur for an increasing velocity front and variations of temperature are strongest during velocity decrease.

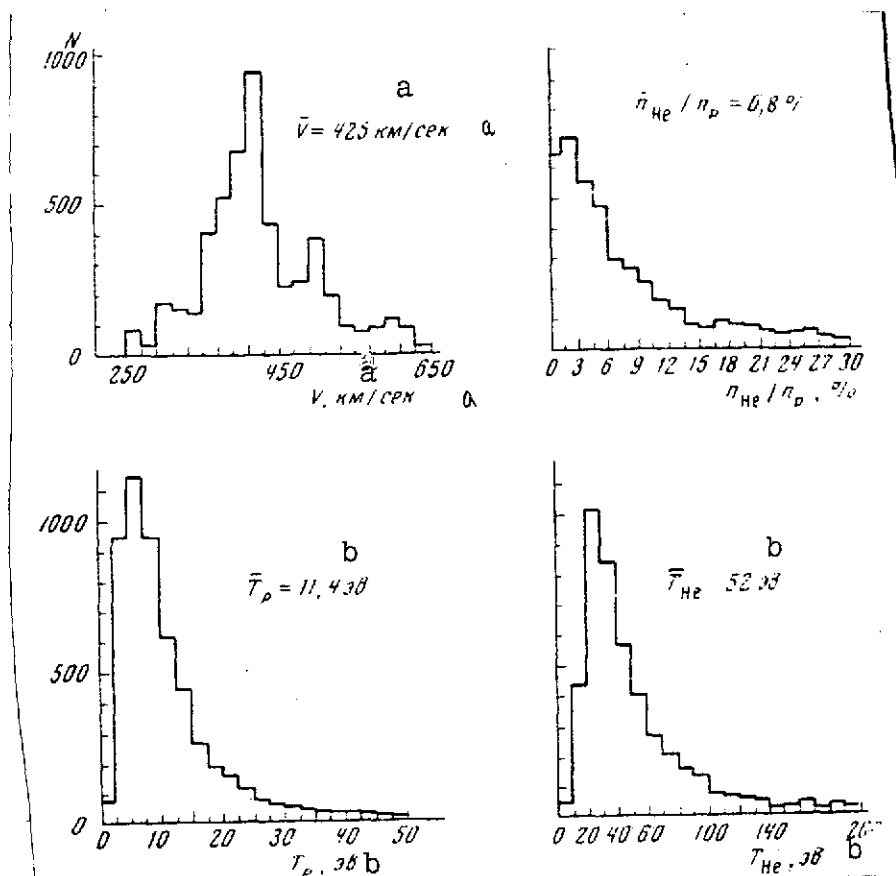


Fig. 3. Histograms of solar wind parameters, built up on the results of measurement onboard the Mars-3 spacecraft from 16 Jun to 21 Aug 1971. Average values are shown in the figure.

Key: a. km/sec
b. ev

In Fig. 3 are shown velocity histograms of solar wind, the temperature of protons and ions of He^{++} , and also the ratio in the concentration of ions of He^{++} to the concentration of protons, measured from 16 Jun to 21 Aug. The velocity histogram shows a multipeak structure, which is caused by the flow structure of solar wind, maintained in a general way during more than three revolutions of the Sun, which occurred during the period of time taken.

The presence of long-life flow formations also appears on temperature histograms, as does the ratio of concentrations, but

they are less marked owing to the great dispersion of the dimensions and the greater errors in their determination.

The average values of parameters on histograms in Fig. 3 was calculated without taking into account the difference in errors of average values of frequency of events in each separate interval of the averaged dimension, which obviously caused an exaggerated average value in the ratio of the concentration of He^{++} to the concentration of ions. In this section, the method described was used for processing a significant part of the information obtained by the Mars-3 spacecraft. /750

Observations of the Geomagnetospheric Trail

During the period from 22 Jul to 8 Aug, an instrument recorded ion spectra, which were quite different from those normally observed on the track of spectra of ions of solar wind. The Mars-3 spacecraft, at that time, had left point A with a geocentric distance of $\approx 2200 R_E$, with an angle of the spacecraft -- Earth -- antisolar point 15° to point B with a geocentric distance of $3400 R_E$ and an angle of spacecraft -- Earth -- antisolar point 9° , where, during this period, the spacecraft was $400 R_E$ lower than the plane of the ecliptic (Fig. 4). The most distinguishing features of spectra observed during this period are: 1) a reduction of 1-2 in the size of ion flows; 2) the appearance of a second maximum in the energy spectrum, comparable in size to the first or even exceeding it; 3) change in the ratio of the position of maxima on the scale from 2, as was observed in solar wind for proton and α -peaks to 3; 4) the variability in the shape of spectra during the measurement time of 1 minute; 5) an increase in the fluctuation of temperature in the flow of ions.

In Fig. 5 are shown some typical spectra of this range. Similar measurement was interpreted earlier in work [9] as an intersection of the Earth's geomagnetic trail.

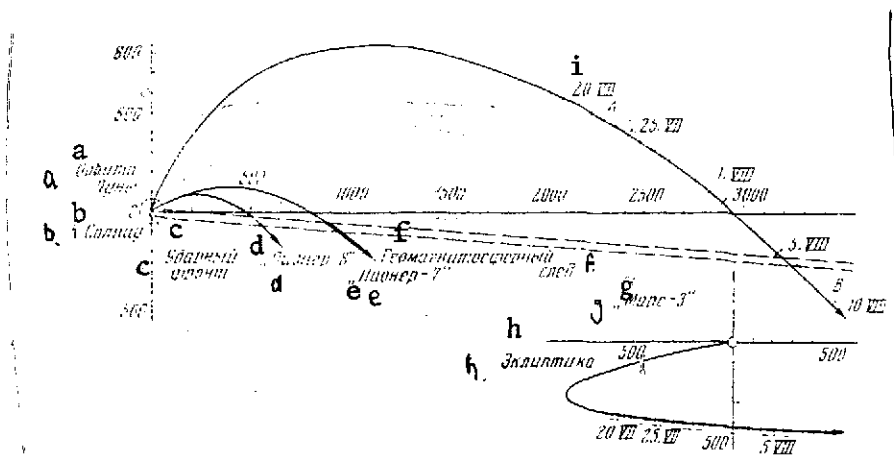


Fig. 4. The trajectory of the Mars-3 spacecraft in solar-ecliptic coordinates with a center on the Earth (above: the projection on the ecliptic plane; below: view from the Sun). Distances are shown in radii of the Earth. The dashed line along the trajectory indicates the range of observation of disturbed spectra, although the relative frequency of their occurrence and the nature of disturbance are different in that area. Trajectories of Pioneer-7 and Pioneer-8 are shown, with the intersection area of the geomagnetospheric trail, the expected continuation of the geomagnetic tail (its thickness is approximately equal to the diameter of the tail in the Moon's orbit) and the position of the shock front with small parameter values.

Key: a. Moon's orbit e. Pioneer-7
 b. To the Sun f. Geomagnetospheric trail
 c. Shock front g. Mars-3
 d. Pioneer-8 h. Ecliptic
 i. 20.VII = 20 Jul [typ.]

Before these measurements, the intersection of the Earth's geomagnetic trail had been observed by two spacecraft, Pioneer-7 and Pioneer-8 [7, 8]. In the Pioneer-7 the phenomena linked with the intersection of the geomagnetospheric trail were recorded at a geocentric distance of $1000 R_E$ and $25-28 R_E$ above the ecliptic plane. Pioneer-8 intersected the geomagnetic trail at a geocentric distance of $500 R_E$, at $8.5-12 R_E$ above the ecliptic plane [8, 10].

The observed spectra of ions in the disturbed zone of the geomagnetospheric trail and variations of the spectra coincide

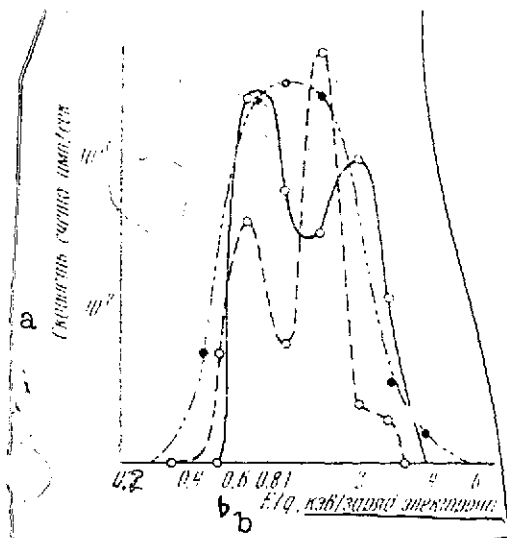


Fig. 5. Three types of disturbed spectra of ions, observed onboard the Mars-3 spacecraft in the geomagnetospheric trail range.

Key: a. Speed count impulses/sec
b. E/q , kev/electron charge

with results obtained by the Pioneer-7 and Pioneer-8. This proves that the character of disturbances in the trail does not significantly change at distances of 500 to 3000 R_E . The presence of two relatively stable maxima in energy distribution, i.e., two velocity streams with significantly different speeds, is difficult to explain within the framework of the normal hydrodynamic model of solar wind.

The length of the disturbance area, which we observed in the trail zone, is significantly greater than follows from the normal hydrodynamic model, where this dimension changes as $z^{1/3}$.

In the trail zone, quite regular fluctuations of velocity of plasma flow were observed, which, in our belief, are linked with the modulation of the flow as a result of the interaction of solar wind with the magnetosphere or Earth's tail. An example of such regular fluctuations is shown in Fig. 6.

Observations in the Vicinity of Mars

The Mars-2 and Mars-3 spacecraft, on 27 Oct and 2 Dec 1971, were shifted from interplanetary trajectories to Mars orbit. When this was done, the orbits of both stations were significantly different. Hence, the maximum distance of Mars-3 was more than 200,000 km from the planet and its orbit period was more than 12 days. The same parameters for Mars-2 were 25,000 km and 17 hours. Both stations passed at a distance of 1300 km from the planet in

7751

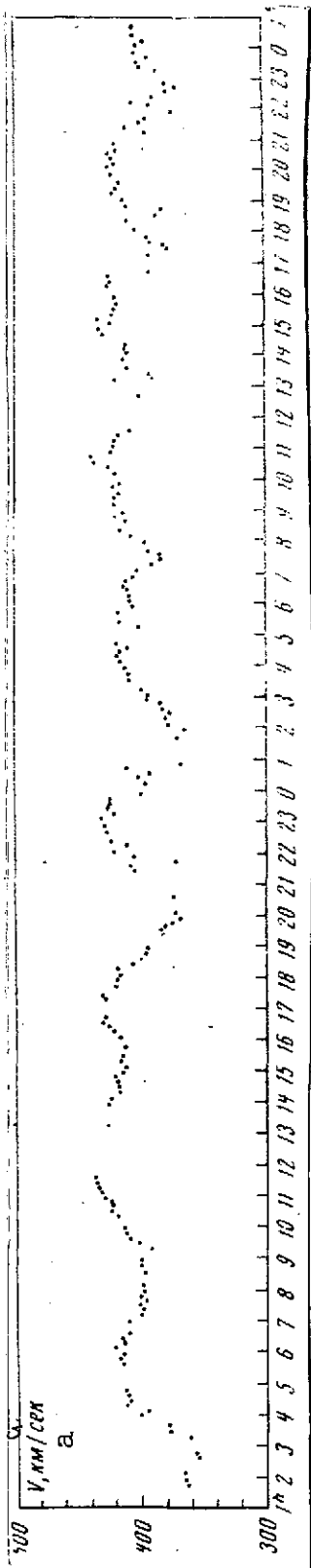


Fig. 6. An example of regular velocity fluctuations (Alveno waves) observed on the Mars-3 spacecraft in the geomagnetospheric trail region.

Key: a. km/sec

the orbit pericenters, although the orbit of Mars-3 underwent evolution changes from revolution to revolution and the smallest distance at first decreased to 1100 km, and then began to increase. During the whole time that Mars-3 was working, the instruments for measuring the flows of ions worked normally and it was possible to obtain data on flows of ions for the period until April 1972. Information obtained by Mars-2 showed that the majority of the instrument channels had a high background noise, which made it impossible to separate signals from particles recorded on those channels. However, the channel measuring the flows of ions in the 0.03-0.17 kev range functioned normally, and this information proved a useful supplement to the results obtained by Mars-3.

During the majority of revolutions, the instrument on Mars-3 measured energy spectra similar to those of solar wind in interplanetary space. There was a change in the character of the flow during all the revolutions of Mars-3 near the pericenter. Here, there was a sharp decrease in the number of ions, with energy in the 0.5-2.5 keV range, and ions in the 0.03-0.15 keV range appeared which had not been observed earlier. Flows of ions in this energy range in solar wind are not normally observed, since the velocity of solar wind does not fall below 250 km/sec, and the temperature is approximately 10 eV. The appearance of ions with an energy of 0.03-0.15 keV regularly in one area of space around a planet shows that the spacecraft intersects the interaction zone of solar wind with Mars. In Fig. 7 are shown examples of energy spectra of ions measured before entering the disturbance zone (curve 1) and in the disturbance zone itself (curve 2). The abrupt increase in velocity and temperature when entering the disturbance zone made it possible to interpret these measurements as the intersection of the collisionless shock wave near Mars [12]. The computed values of sharp rises in velocity and temperature on the observed spectra (see Fig. 7), allowing for uncertainty in the Mach number M and in the adiabatic index γ , do not conflict with theoretical calculations, based on a hydrodynamic model of flow around an obstruction [3, 16].

The subsequent investigation was done on the supposition that the area of flow around Mars, in the first approximation, is axially symmetrical to the line from Mars to the Sun. In Fig. 8 are shown observation points of the spectrum, characteristic of the transient area in the cylindrical coordinates system. The external boundary of this zone shows the position of the shock wave in relation to the planet. The internal boundary of the zone on the diagram does not correspond to the actual boundary of the streamlined obstruction, since, firstly, the Mars-3 orbit was quite far from the shadow area and, secondly, on those parts of

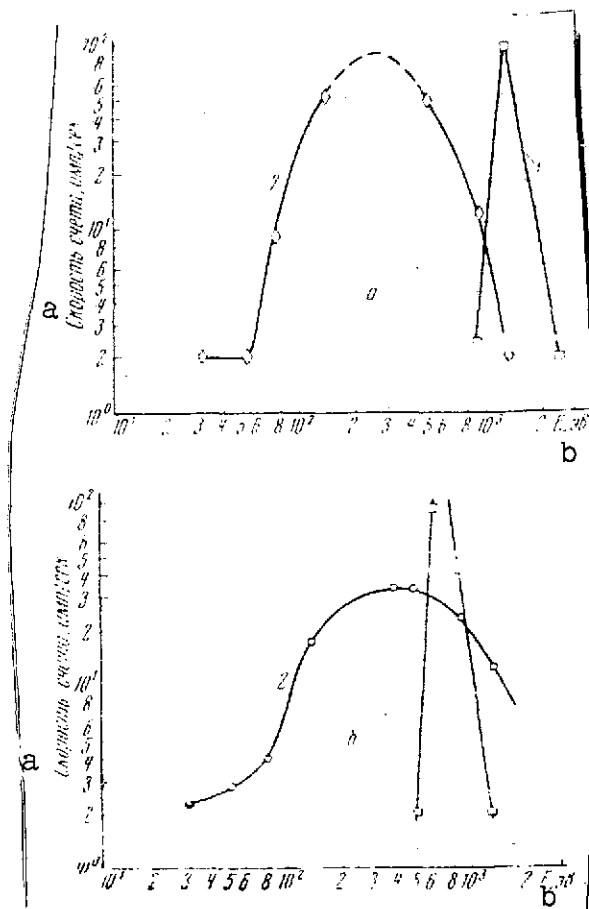


Fig. 7. Examples of sharp rises in velocity and temperature on a departing shock wave near Mars. 1 - free flow of ions; 2 - flow of ions behind the shock wave. Calculated values of speed and temperature: a - 9 Jan 1972, $V_1 \sim 500$ km/sec; $T_1 \leq 15$ ev; $V_2 = 290$ km/sec; $T_2 = 120$ ev; b - 3 Feb 1972, $V_1 \sim 450$ km/sec; $T_1 \leq 20$ ev; $V_2 = 220$ km/sec, $T_2 = 100$ ev.

Key: a. Count speed, impulses/sec
b. E, ev

the trajectory approaching the planet, instruments for plasma measurement are usually switched off, in favor of instruments used for measuring the Martian surface.

On 21 Jan 1972, when Mars-3 passed closest to the surface, at ~ 1130 km, equipment for measuring plasma and the magnetic field was switched on when passing the whole of the periarion with a 2 min interrogation cycle in order to obtain more accurate information. In Fig. 8, those parts of the trajectory which are within the shock wave are marked with a dashed line; the part of the trajectory when Mars' magnetic field was passed is indicated by a solid line (see [17]).

The average position of the front of the shock wave, obtained by observing plasma, corresponds to the position of any point of an obstruction ~ 1000 km above the Martian surface. This, as was said earlier [13], is significantly higher than can be obtained by gasokinetic pressure of the ionosphere. In this way, our

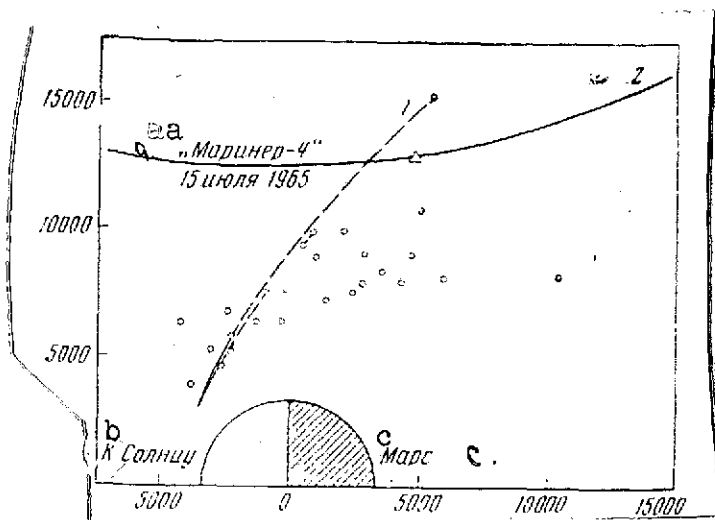


Fig. 8. Observations from Mars-3 of a spectrum typical of a transient area, shown in areocentric cylindrical coordinates with the axis directed towards the Sun. The coordinates of observation points in December 1971 and April 1972 are shown by small circles. 1 - the trajectory of Mars-3 21 Jan 1972, when more detailed measurement was done; dashed lines - parts of the trajectory, corresponding to the transient area; solid line - the area of intensified observation near Mars' magnetic field; 2 - the trajectory of Mariner-4; the suggested intersection of the departing shock wave is shown by a triangle.

Key: a. Mariner-4, 15 Jul 1965
b. Towards the Sun
c. Mars

The position of the shock wave near Mars fluctuated considerably. In Fig. 8 the point in the transient area can be seen during the day, approximately twice as far from the Martian surface, than the average position of the shock wave. Information from Mars-2, which intersected the shock wave several hours before Mars-3, also showed that, during this time, the shock wave was farther away than normal.

information on the significant dimension of the obstruction has something in common with measurements of Mars' magnetic field at altitudes greater than 1100 km [17].

In Fig. 9 is shown the power spectrum of ions measured while the magnetic field of Mars was being passed. The corresponding temperature of ions is approximately 20 ev, and the concentration, calculated on the assumption of isotropic distribution, is approximately 10 cm^{-3} . It would be interesting to find out whether these particles are a special type of trapped radiation.

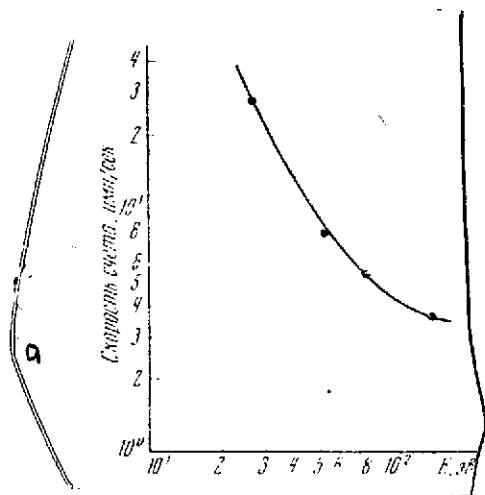


Fig. 9. Power spectrum of ions observed on 21 Jan 1972 in the intensified magnetic area near Mars. Evaluation of parameters: T_p 20 ev, n_p = 10 cm.

Key: a. Count rate,
impulses/sec
b. ev

In Fig. 8 is also shown that part of the trajectory of Mariner-4 on a Mars flight on 15 July 1965 [2]. The point for the possible intersection of the shock wave, determined by measuring the magnetic field, is marked with a triangle. It can be seen that measurement carried out by Mars-3 does not conflict with the possibility that Mariner-4 intersected the departing shock wave near Mars. In this way,

In this way, measurement carried out made it possible, firstly, to ascertain the existence of a departing shock wave near Mars. By the sudden rise in velocity and temperature during the gap, this shock wave, apparently, corresponds to the theoretical calculations [4, 16] and the departing shock wave near the Earth's magnetosphere [18]. Some anomalies in the power spectrum were observed in the free flow near Mars, before the shock wave [13], which can be linked with the fact that the departing shock wave is inside the areocorona [19]. However, further analysis of experimental data is required to confirm this occurrence.

A second conclusion from the material shown is that the departing shock wave is formed farther from Mars than follows from the supposition on the balance of pressure of a flow of solar wind and ionospheric plasma [4]. This can indicate that either the dimension of the obstruction is greater than was supposed (which, at first glance, agrees with measurement of magnetic field by Mars-2 and Mars-3 [17]), or the external

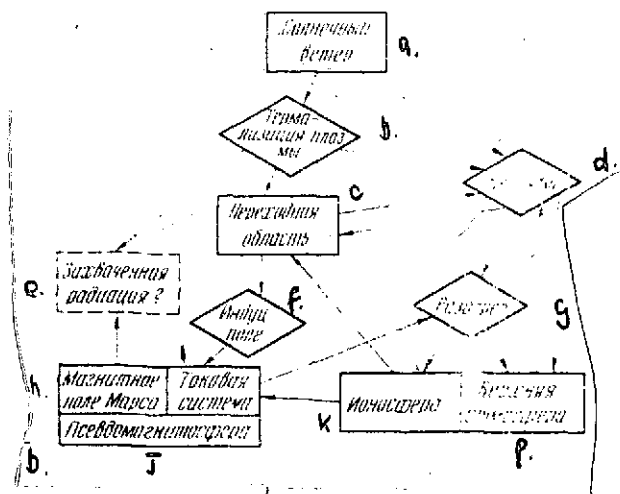


Fig. 10. A diagram of processes of solar wind flowing around Mars. See explanations in text.

- Key:
- a. Solar wind
 - b. Plasma thermalization
 - c. Transient area
 - d. Recharging
 - e. Trapped radiation?
 - f. Induction field
 - g. Warming-up
 - h. Martian magnetic field
 - i. Current system
 - j. Pseudomagnetosphere
 - k. Ionosphere
 - l. Upper atmosphere

atmosphere of Mars has an influence on plasma flow parameters, as was suggested in work [20].

The question linked with 7754 the magnetic field near the planet, is quite complicated, since the electric field induced into the Martian ionosphere must energize ionospheric currents [6]. The electrical link of solar wind with the ionosphere is brought about by the diffusion of particles of solar wind into the area with an increased magnetic field near the planet. The overall size of the magnetic field is determined by the speed of diffusion of solar wind and the dissipation of ionospheric

currents. The posing of the problem and methods for solving it are given in work [6]; however, the problem still needs to be solved, and the contribution of an induced magnetic field into the observed area near Mars is not known.

In Fig. 10 is given a schematic presentation of phenomena near Mars. Rectangles indicate areas or formations, diamond shapes -- processes, arrows -- possible links. At the present time there is a preliminary picture of the structure of space near Mars and indications of some processes in it. More detailed analysis

must be carried out into observations, and also further study of plasma phenomena with measurement of magnetic and electric fields and plasma, especially, of ion and mass composition of hot plasma.

The authors are grateful to R.A. Isayeva for help in processing the experimental data.

REFERENCES

1. Lazarus, A.J., H.S. Bridge, J.M. Davis, and S.W. Snyder, Space Res. VII, 1296 (1967).
2. Smith, E.J., L. Davis, Jr., P.J. Coleman, Jr., and D.E. Jones, Science 149/3689, 1241 (1965).
3. Dryer, M. and G.R. Heckman, Solar Phys. 2/1, 112 (1967).
4. Spreiter, J.R., A.L. Summers, and A.W. Rizzi, Planet. Space Sci. 18/9, 1281 (1970).
5. Kliore, A., D.L. Cain, G.S. Levy, V.R. Eshleman, G. Fjeldbo, and F. Drake, Science 149/3689, 1243 (1965).
6. Johnson, F.S. and J.E. Midgley, "Induced magnetosphere of Venus," COSPAR 11, Tokyo, (May 1968).
7. Wolfe, J.H., R.W. Silva, D.D. McKibbin, and R.H. Mason, J. Geophys. Res. 72/17, 4577 (1967). /755
8. Intriligator, D.S., J.H. Wolfe, D.D. McKibbin, and H.R. Collard, Planet. Space Sci. 17/3, 321 (1969).
9. Intriligator, D.S., J.H. Wolfe, and D.D. McKibbin, J. Geophys. Res. 77/25, 4645 (1972).
10. Siskoe, G.L., F.L. Scart et al., J. Geophys. Res. 75/28, 5391 (1970).
11. Vaysberg, O.L., A.V. Bogdanov et al., Dokl. AN SSSR 203/2, 309 (1972).
12. Vaysberg, O.L., A.V. Bogdanov et al., Kosmich. issled. 10/3, 462 (1972).
13. Vaysberg, O.L., A.V. Bogdanov et al., Icarus 18, 59 (1973).
14. Hundhausen, A.J., Rev. Geophys. and Space Phys. 8/4, 729 (1970).
15. Hundhausen, A.J., J.T. Gosling, J.R. Asbridge, and V. Pizzo, J. Geophys. Res. 77/28, 5442 (1972).
16. Dryer, M., Cosmic Electrodynamics 1/2, 115 (1970).
17. Dolginov, Sh.Sh., Ye.G. Yeroshenko, and L.I. Zhuzgov, Dokl. AN SSSR 207/6 (1972).
- 18.

18. Argo, H.V., J.R. Asbridge, S.J. Bame, A.J. Hundhausen, and J.B. Strong, J. Geophys. Res. 72/7, 1989 (1967).
19. Dementyeva, N.N., V.G. Kurt, A.S. Smirnov, L.G. Titarchuk, and S.D. Chuvahin, Preprint IKL D 139, Moscow, 1972.
20. Wallis, M.K., Cosmic Electrodynamics 3/1, 45 (1972).